

Synthesis and Evaluation of Photoluminescent and Electrochemical Properties of New Aromatic Polyamides and Polyimides with a Kink 1,2-Phenylenediamine Moiety

GUEY-SHENG LIOU, YI-LUNG YANG, YUHLONG OLIVER SU

Department of Applied Chemistry, National Chi Nan University, 1 University Road, Nantou Hsien 545, Taiwan, Republic of China

Received 23 December 2005; accepted 28 January 2006

DOI: 10.1002/pola.21358

Published online in Wiley InterScience (www.interscience.wiley.com).

ABSTRACT: A series of novel triphenylamine-containing aromatic polyamides and polyimides having a crank and twisted noncoplanar structures were synthesized in inherent viscosities of 0.14–0.64 dL/g and 0.11–0.67 dL/g, respectively. These polymers had useful levels of thermal stability associated with relatively high glass-transition temperatures (174–311 °C). They exhibited strong UV–Vis absorption bands at around 300 nm in NMP solutions. The PL spectra of these polymers in NMP solutions (1×10^{-5} M) showed maximum peaks around 396–479 nm. The hole-transporting and electrochromic properties were examined by electrochemical and spectroelectrochemical methods. Cyclic voltammetry (CV) of the polymer films cast onto an indium-tin oxide (ITO)-coated glass substrate exhibited two reversible oxidation redox couples at potentials of 0.70–1.01 V and 1.10–1.46 V, respectively, vs. Ag/AgCl in acetonitrile solution. The polymer films revealed electrochromic characteristics, with a color change from neutral pale yellowish to green and then to a blue oxidized form at applied potentials ranging from 0.00 to 1.75 V. © 2006 Wiley Periodicals, Inc. *J Polym Sci Part A: Polym Chem* 44: 2587–2603, 2006

Keywords: aromatic polyamides; electrochromic; hole-transporting; *N,N*-bis(4-aminophenyl)-*N,N'*-diphenyl-1,2-phenylenediamine; poly(amine amide)s; poly(amine imide)s; polyimides; triphenylamine

INTRODUCTION

Triphenylamine (TPA) and its derivatives have been extensively made as hole-transporting layers (HTLs) in organic light-emitting diodes (OLED) devices because of their high carrier mobility, low ionization potentials, and amorphous film-forming ability.^{1–6} However, the morphological change resulting from deposited heat during processing and molecular migration promoted by the molecular motion near glass-transition temperature (T_g)

would degrade the electroluminescence (EL) devices and then shorten their lifetime. Therefore, high T_g 's and high molecular weights of HTL materials are required for the long-term stability of the EL devices. In recent years, intensive research efforts have been focused on the development of new charge-transport polymers because they promise a number of commercial advantages over low-molecular-weight counterparts. The feasibility of using spin-coating and ink-jet printing processes for large-area EL devices and the possibilities of various chemical modifications (to improve emission efficiencies and allow patterning) make polymeric materials containing triarylamine units very attractive.^{7–13} To enhance the hole-injection ability of polymeric emissive materials such as poly

Correspondence to: G.-S. Liou (Email: gsliau@ncnu.edu.tw) or Y. O. Su (E-mail: yosu@ncnu.edu.tw)

Journal of Polymer Science: Part A: Polymer Chemistry, Vol. 44, 2587–2603 (2006)
© 2006 Wiley Periodicals, Inc.

(1,4-phenylenevinylene)s (PPVs) and polyfluorenes (PFs), there have been several reports on PPV and PF derivatives involving hole-transporting units such as triarylamine or carbazole groups in the emissive π -conjugated core/main chains^{14–21} or grafting them as side chains in a polymer^{22–25} or attaching them onto the polymer chain ends or the outer surface of dendritic wedges.^{26,27}

Aromatic polyamides and polyimides are well accepted as advanced materials for thin-film applications in microelectronic devices and liquid-crystal displays because of their outstanding mechanical, chemical, thermal, and physical properties.^{28,29} However, the technological applications of most of these polymers are limited by processing difficulties because of high melting temperatures or T_g 's and limited solubility in most organic solvents because of their rigid backbones. To overcome these limitations, polymer-structure modification becomes necessary. One of the common approaches for increasing the solubility and processability of polyamides and polyimides without sacrificing their high thermal stability is the introduction of bulky, packing-disruptive groups and/or kink structures into the polymers.^{30–40} Recently, we reported the synthesis of soluble aromatic polyamides and polyimides bearing TPA units in the main chain based on *N,N'*-bis(4-aminophenyl)-*N,N'*-diphenyl-1,4-phenylenediamine,^{41,42} *N,N*-bis(4-aminophenyl)-*N',N'*-diphenyl-1,4-phenylenediamine,^{43,44} and *N,N*-bis(4-carboxyphenyl)-*N',N'*-diphenyl-1,4-phenylenediamine.^{45,46} Because of the incorporation of bulky, three-dimensional propeller-shaped TPA units along the polymer backbone, all the polymers were amorphous, had good solubility in many aprotic solvents and good film-forming capability, and exhibited high thermal stability.

The electrochemistry of TPA in aprotic solvents has been well studied.⁴⁷ The TPA cationic radical of the first electron oxidation is not stable, and the chemical reaction therefore follows up to produce tetraphenylbenzidine by tail-to-tail (para positions) coupling with the loss of two protons per dimer. In our previous study, it was also observed that the phenyl groups were incorporated by electron-donating substituents at the para position of triarylamines and the coupling reactions were greatly prevented, and this afforded stable cationic radicals.^{48,49} In this article, we describe the synthesis of a novel aromatic diamine monomer having a crank and twisted noncoplanar structure, *N,N*-bis(4-aminophenyl)-*N,N*-diphenyl-1,2-phenylenediamine (**4**), and its

derived poly(amine amide)s and poly(amine imide)s containing electron-rich TPA groups with diphenylamine ortho-substituted on the pendent phenyl ring. The general properties, such as the solubility, crystallinity, and thermal properties, are described. The electrochemical, electrochromic, and photoluminescence (PL) properties of these polymers are also investigated here.

EXPERIMENTAL

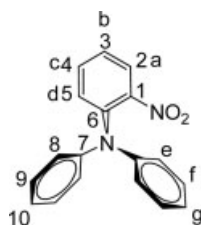
Materials

According to well-known chemistry, 2-aminodiphenylamine (**2**; mp = 151–153 °C) was prepared by the aromatic nucleophilic amination of 2-nitrofluorobenzene and diphenylamine in *N,N*-dimethylformamide (DMF) in the presence of sodium hydride, followed by reduction by means of hydrazine and Pd/C in refluxing ethanol. Diphenylamine (Lancaster), 2-fluoronitrobenzene (Acros), 4-fluoronitrobenzene (Aldrich), sodium hydride (95%; dry; Aldrich), 10% Pd/C (Lancaster), and hydrazine monohydrate [Tokyo Chemical Industry (TCI)] were used as received. *N,N*-Dimethylacetamide (DMAc; Tedia), DMF (Acros), *N*-methyl-2-pyrrolidinone (NMP) (Tedia), pyridine (Py; Tedia), and triphenyl phosphite (TPP; Acros) were also used as received. Commercially available aromatic dicarboxylic acids such as terephthalic acid (**5a**; TCI), isophthalic acid (**5b**; TCI), 2,6-naphthalenedicarboxylic acid (**5c**; TCI), 4,4'-diphenyldicarboxylic acid (**5d**; TCI), 4,4'-oxydibenzoic acid (**5e**; TCI), 4,4'-sulfonyldibenzoic acid (**5f**; TCI), acetylenedicarboxylic acid (**5g**; TCI), and *trans*-1,4-cyclohexanedicarboxylic acid (**5h**; TCI) were used as received. Available aromatic tetracarboxylic dianhydrides such as pyromellitic dianhydride (**7a**; Chriskev), 3,3',4,4'-benzophenone tetracarboxylic dianhydride (**7c**; Chriskev), 4,4'-oxydiphthalic dianhydride (**7d**; TCI), and 3,3',4,4'-diphenyl sulfone-tetracarboxylic dianhydride (**7e**; TCI) were purified by recrystallization from acetic anhydride. 3,3',4,4'-Biphenyltetracarboxylic dianhydride (**7b**; Chriskev), 2,2-bis(3,4-dicarboxyphenyl) hexafluoropropane dianhydride (**7f**; Chriskev), and 1,2,3,4-cyclopentanetetracarboxylic dianhydride (**7g**; TCI) were purified by vacuum sublimation. Tetra-*n*-butylammonium perchlorate (TBAP) was obtained from Acros and recrystallized twice from ethyl acetate and then dried *in vacuo* before use. All other reagents were used as received from commercial sources.

Preparation of 2-Nitrotriphenylamine (1)

A mixture of 5.08 g (0.21 mol) of sodium hydride in 250 mL of DMF was stirred at room temperature. To the mixture, 32.85 g (0.20 mol) of diphenylamine and 28.36 g (0.201 mol) of 2-fluoronitrobenzene were added in sequence. The mixture was heated with stirring at 120 °C for 20 h and then precipitated into 2.5 L of a saturated NaCl aqueous solution. Recrystallization twice from methanol yielded 38.63 g of the desired dinitro compound (**1**) as orange-red needles in a 67% yield.

mp: 102–104 °C [differential scanning calorimetry (DSC) at a scanning rate of 10 °C/min]. IR (KBr): 1590, 1356 cm^{-1} (NO_2 stretch). ^1H NMR [dimethyl sulfoxide- d_6 (DMSO- d_6), δ , ppm]: 7.89 (d, 1H, H_a), 7.66 (t, 1H, H_c), 7.36 (t, 1H, H_b), 7.30 (d, 1H, H_d), 7.26 (t, 4H, H_f), 7.02 (t, 2H, H_g), 6.90 (d, 4H, H_e). ^{13}C NMR (DMSO- d_6 , δ , ppm): 139.9 (C^1), 134.6 (C^7), 130.2 (C^6), 129.6 (C^9), 126.2 (C^4), 126.0 (C^3), 125.7 (C^5), 123.4 (C^{10}), 122.6 (C^8), 122.5 (C^2). ELEM. ANAL. Calcd. for $\text{C}_{18}\text{H}_{14}\text{N}_2\text{O}_2$ (290.32): C, 74.47%; H, 4.86%; N, 9.65%. Found: C, 74.22%; H, 5.03%; N, 9.69%.

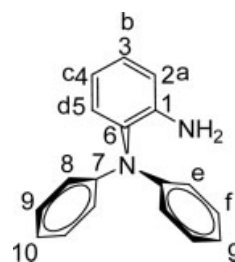


Preparation of 2-Aminotriphenylamine (2)

In a 250-mL, round-bottom flask, 4.00 g (13.78 mmol) of dinitro compound **1** and 0.1 g of 10% Pd/C were added to 60 mL of ethanol. After the addition of 2 mL of hydrazine monohydrate, the solution was stirred at the reflux temperature for 9 h. After the solution cooled to room temperature, the solvent was removed from the filtrate under reduced pressure. The residue was purified by recrystallization from ethanol/water, and the finally purified product (**2**) as light pink needles was dried *in vacuo* at 95 °C. The yield was 2.70 g (75%).

mp: 151–153 °C (DSC, 10 °C/min). IR (KBr): 3473, 3378 cm^{-1} (NH_2 stretch). ^1H NMR (CDCl_3 , δ , ppm): 7.2 (t, 4H, H_f), 7.08–7.10 (m, 2H, $\text{H}_c + \text{H}_d$), 7.00 (d, 4H, H_e), 6.84 (t, 2H, H_g), 6.83 (d, 1H, H_a), 6.78 (t, 1H, H_b), 3.76 (s, 2H, $-\text{NH}_2$). ^{13}C NMR (CDCl_3 , δ , ppm): 146.7 (C^7), 142.8 (C^1), 132.5 (C^6), 130.1 (C^4), 129.2 (C^9), 127.1 (C^3), 121.9 (C^{10}), 121.3 (C^8), 118.8 (C^5), 117.1 (C^2). ELEM. ANAL. Calcd. for

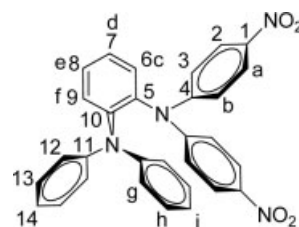
$\text{C}_{18}\text{H}_{16}\text{N}_2$ (260.33): C, 83.04%; H, 6.19%; N, 10.76%. Found: C, 83.10%; H, 6.06%; N, 10.56%.

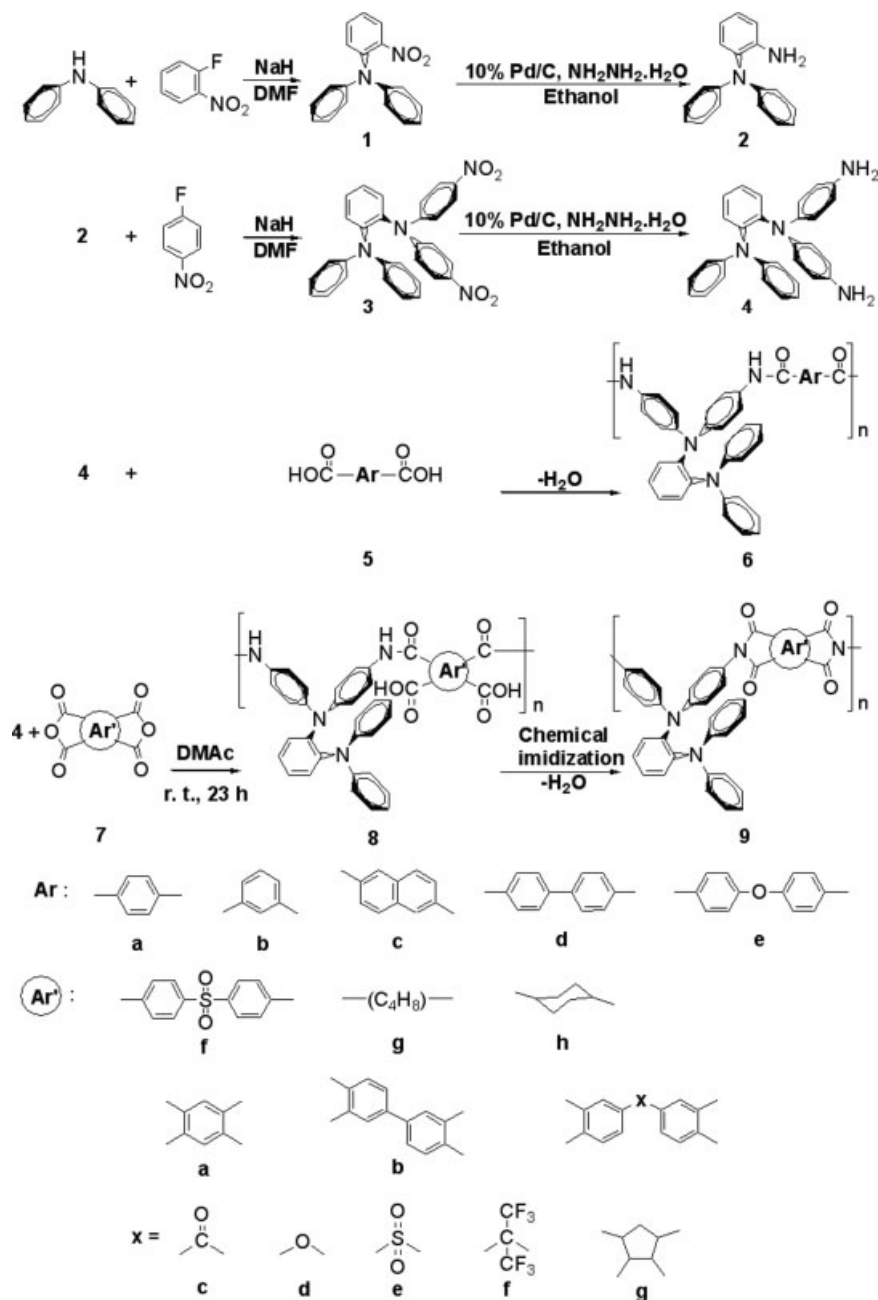


Preparation of *N,N*-Bis(4-nitrophenyl)-*N'*,*N'*-diphenyl-1,2-phenylenediamine (3)

A mixture of 4.48 g (0.177 mol) of sodium hydride in 200 mL of DMF was stirred at room temperature. To the mixture, 23.08 g (0.0886 mol) of **2** and 25.02 g (0.177 mol) of 4-fluoronitrobenzene were added in sequence. The mixture was heated with stirring at 120 °C for 20 h and then precipitated into 2.5 L of a saturated NaCl aqueous solution. Recrystallization from acetonitrile yielded 24.60 g of the desired dinitro compound **3** as orange crystals in a 55% yield.

mp: 186–189 °C (DSC, 10 °C/min). IR (KBr): 1581, 1342 cm^{-1} ($-\text{NO}_2$ stretch). ^1H NMR (DMSO- d_6 , δ , ppm): 7.34 (d, 4H, H_b), 7.31 (d, 4H, H_a), 7.18–7.20 (t, 2H, $\text{H}_d + \text{H}_e$), 7.13 (t, 4H, H_h), 6.93 (d, 4H, H_g), 6.91 (t, 2H, H_i), 6.65–6.67 (d, 2H, $\text{H}_c + \text{H}_f$). ^{13}C NMR (DMSO- d_6 , δ , ppm): 151.7 (C^1), 150.8 (C^4), 146.5 (C^5), 142.1 (C^{11}), 140.0 (C^{10}), 129.2 (C^{13}), 125.7 (C^{14}), 125.0 (C^{12}), 123.1 (C^9), 123.0 (C^7), 122.7 (C^2), 122.4 (C^8), 122.3 (C^6), 122.0 (C^3). ELEM. ANAL. Calcd. for $\text{C}_{30}\text{H}_{22}\text{N}_4\text{O}_4$ (502.52): C, 71.70%; H, 4.41%; N, 11.15%. Found: C, 71.54%; H, 4.49%; N, 11.08%. Crystal data: yellow crystal grown during slow crystallization in acetonitrile (0.25 × 0.20 × 0.15 mm), monoclinic $\text{C}2/c$ with $a = 34.0537(10)$ Å, $b = 9.2088(3)$ Å, $c = 16.8807(3)$ Å; $\alpha = 90^\circ$, $\beta = 93.878(2)^\circ$, and $\gamma = 90^\circ$, where the density of the crystal was 1.264 Mg/m^3 for $Z = 8$ and $V = 5281.6(2)$ Å³.





Scheme 1. Monomer and polymer synthesis.

Preparation of *N,N*-Bis(4-aminophenyl)-*N'*,*N'*-diphenyl-1,2-phenylenediamine (4)

In a 250-mL, round-bottom flask, 2.40 g (4.76 mmol) of dinitro compound **3** and 0.07 g of 10% Pd/C were added in 40 mL of ethanol. After the addition of 1.2 mL of hydrazine monohydrate, the solution was stirred at the reflux temperature for 14 h. After the solution cooled to room temperature, 40 mL of tetrahydrofuran (THF) was then

added to the suspension solution to dissolve the solid product. The solution was filtered to remove the catalyst, and the filtrate was distilled to remove the solvent. The crude product was purified by recrystallization from toluene to give 1.56 g (74%) of diamine **4** as white crystals.

mp: 219–222 °C (DSC, 10 °C/min). IR (KBr): 3437, 3342 cm^{-1} (NH_2 stretch). ^1H NMR (DMSO- d_6 , δ , ppm): 7.02 (t, 4H, H_b), 7.00 (t, 1H, H_e), 6.90–6.94 (d, 2H, $\text{H}_c + \text{H}_d$), 6.85–6.88 (t, 3H, $\text{H}_f +$

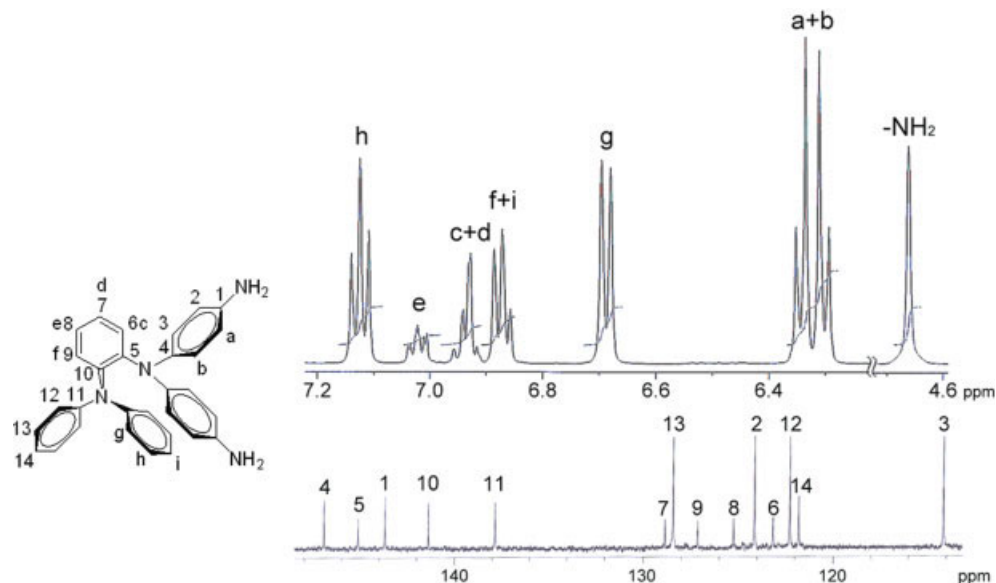
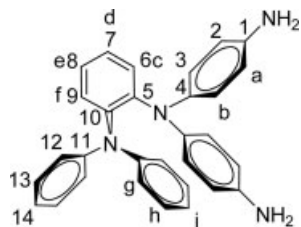


Figure 1. ^1H and ^{13}C NMR spectra of diamine monomer **4** in $\text{DMSO-}d_6$.

H_i), 6.67 (d, 4H, H_g), 6.27–6.34 (d, 8H, H_{a+} H_b), 4.65 (s, 4H, $-\text{NH}_2$). ^{13}C NMR ($\text{DMSO-}d_6$, δ , ppm): 147.1 (C^4), 145.3 (C^5), 143.9 (C^1), 141.6 (C^{10}), 138.0 (C^{11}), 129.0 (C^7), 128.6 (C^{13}), 127.3 (C^9), 125.4 (C^8), 124.3 (C^2), 123.3 (C^6), 122.4 (C^{12}), 122.0 (C^{14}), 114.3 (C^3). ELEM. ANAL. Calcd. for $\text{C}_{30}\text{H}_{26}\text{N}_4$ (442.55): C, 81.42%; H, 5.92%; N, 12.66%. Found: C, 81.64%; H, 5.98%; N, 12.52%



Preparation of Poly(amine amide) **6e** by Direct Polycondensation via the Phosphorylation Reaction

A mixture of 0.443 g (1.00 mmol) of monomer **4**, 0.258 g (1.00 mmol) of **5e**, 0.2 g of calcium chloride, 0.6 mL of TPP, 0.9 mL of Py, and 3 mL of NMP was heated with stirring at 105 °C for 3 h. The polymer solution was poured slowly into 300 mL of stirring methanol, giving rise to a stringy, fiber-like precipitate that was collected by filtration, washed thoroughly with hot water and methanol, and dried at 100 °C; the yield was 0.599 g (90%). Precipitations from DMAc into methanol were carried out twice for further purification. The inherent viscosity of the obtained poly(amine amide)

(**6e**) was 0.58 dL/g, measured at a concentration of 0.5 g/dL in DMAc at 30 °C. The IR spectrum of **6e** (film) exhibited characteristic amide absorption bands at 3309 (N–H stretching), 1664 (amide carbonyl), and 1238 cm^{-1} (ether stretching).

ELEM. ANAL. Calcd. for $(\text{C}_{44}\text{H}_{32}\text{N}_4\text{O}_3)_n$ (664.75) $_n$: C, 79.50%; H, 4.85%; N, 8.43%. Found: C, 78.66%; H, 5.03%; N, 8.56%.

The other poly(amine amide)s were prepared by an analogous procedure.

Preparation of Poly(amine imide) **9d** by a Two-Step Method via a Chemical Imidization Reaction

Monomer **4** (0.553 g, 1.25 mmol) was dissolved in 10 mL of DMAc in a 50-mL, round-bottom flask. Then, **7d** (0.388 g, 1.25 mmol) was added to the diamine solution in one portion. Thus, the solid content of the solution was approximately 10 wt %. The mixture was stirred at room temperature for about 20 h to yield a viscous poly(amic acid) solution. The inherent viscosity of the resulting poly(amic acid) was 0.93 dL/g, measured in DMAc at a concentration of 0.5 g/dL at 30 °C. The precursor poly(amic acid) was subsequently chemically imidized in solution to give the polyimide. A mixture of acetic anhydride (5 mL) and Py (2 mL) was added to the aforementioned poly(amic acid) **8d** solution, and the reaction mixture was stirred at room temperature overnight and at 100 °C for 2 h. After cooling to room temperature, the polymerization mixture was poured slowly into 300 mL of stirred

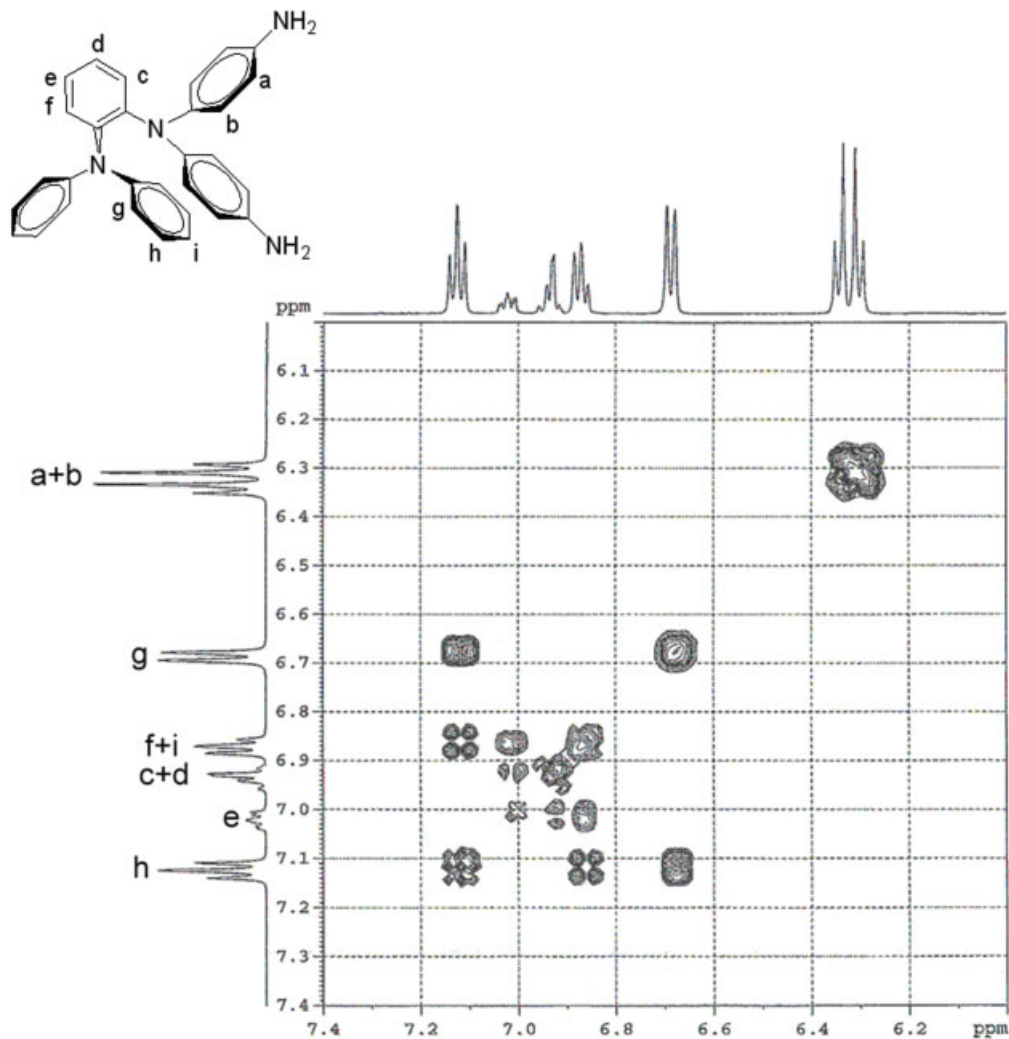


Figure 2. H-H correlation spectroscopy spectrum of compound 4 in DMSO- d_6 .

methanol, giving rise to a fibrous precipitate of poly(amine imide) **9d**, which was collected by filtration, washed thoroughly with methanol, and dried at 100 °C; the yield was 0.892 g (99%). Precipitations from DMAc into methanol were carried out twice for further purification. The inherent viscosity of the obtained poly(amine amide) (**9d**) was 0.65 dL/g, measured at a concentration of 0.5 g/dL in DMAc at 30 °C. The IR spectrum of **9d** (film) exhibited characteristic imide absorption bands at 1775 (asymmetrical carbonyl stretching), 1723 (symmetrical carbonyl stretching), 1240 (ether stretching), and 742 cm^{-1} (imide ring deformation).

ELEM. ANAL. Calcd. for $(\text{C}_{46}\text{H}_{28}\text{N}_4\text{O}_5)_n$ (716.74) $_n$: C, 77.08%; H, 3.94%; N, 7.82%. Found: C, 76.20%; H, 3.84%; N, 7.90%.

The other poly(amine imide)s were prepared by an analogous procedure.

Preparation of the Films

A polymer solution was made by the dissolution of about 0.7 g of the polymer sample in 10 mL of DMAc. The homogeneous solution was poured into a 9-cm glass Petri dish, which was placed in a 90 °C oven overnight for the slow release of the solvent, and then the film was stripped off from the glass substrate and further dried *in vacuo* at 160 °C for 8 h. The obtained films were used for inherent viscosity tests, solubility tests, and PL, electrochemical, and thermal property analyses.

Measurements

IR spectra were recorded on a PerkinElmer RXI Fourier transform infrared spectrometer. Ele-

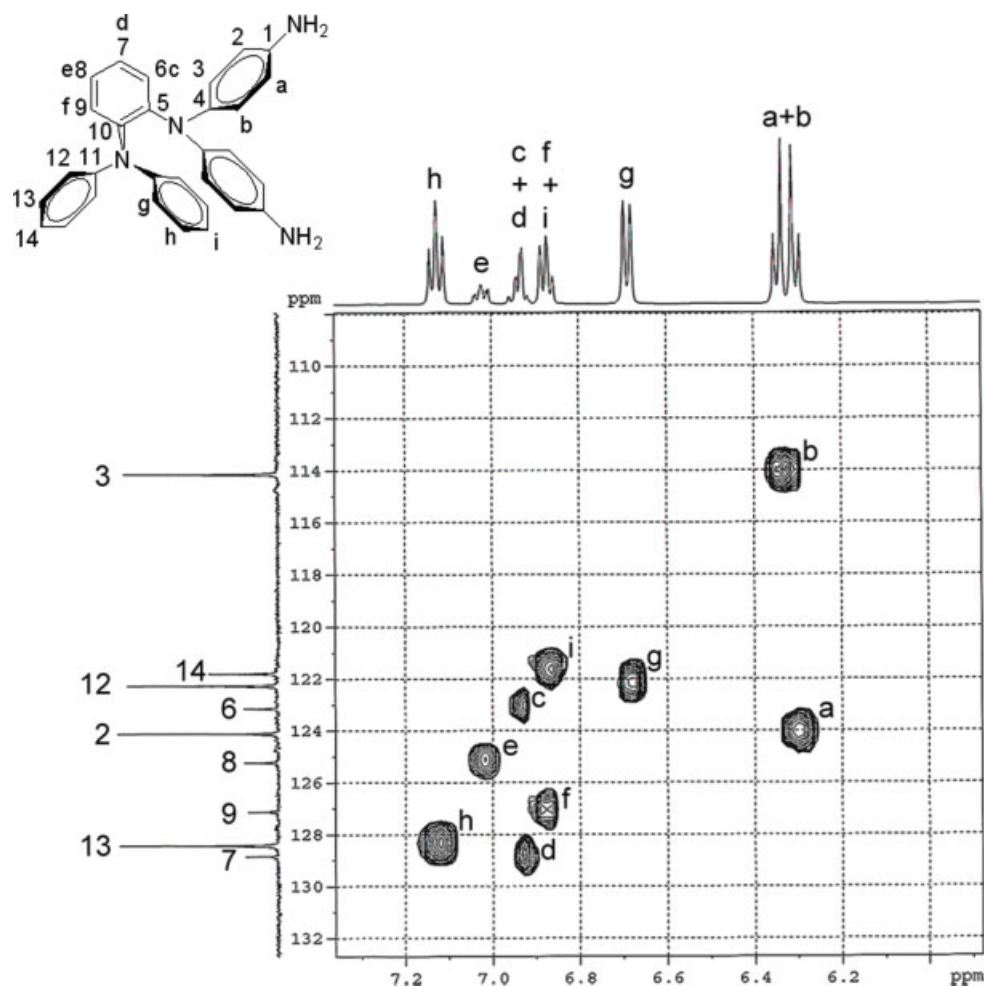


Figure 3. C–H heteronuclear multiple quantum correlation spectrum of compound **4** in DMSO- d_6 .

mental analyses were run in a Elementar Vario EL-III. ^1H and ^{13}C NMR spectra were measured on a Varian Unity Inova 600 FT-NMR system. The inherent viscosities were determined at a 0.5 g/dL concentration with a Tamson TV-2000 viscometer at 30 °C. Ultraviolet–visible (UV–vis) spectra of the polymer films were recorded on a Varian Cary 50 probe spectrometer. DSC analyses were performed on a PerkinElmer Pyris Diamond DSC instrument at a scanning rate of 20 °C/min in flowing nitrogen (20 cm³/min). Electrochemistry was performed with a Bioanalytical System model CV-27 potentiostat and a BAS X–Y recorder. Cyclic voltammetry (CV) was conducted with the use of a three-electrode cell in which indium tin oxide (ITO; polymer film area \approx 0.7 cm \times 0.5 cm) was used as a working electrode. A platinum wire was used as an auxiliary electrode. All cell potentials were taken

with a home-made Ag/AgCl, KCl (saturated) reference electrode. The spectroelectrochemical cell was composed of a 1-cm cuvette, ITO as a working electrode, a platinum wire as an auxiliary electrode, and a Ag/AgCl reference electrode. Absorption spectra were measured with an HP 8453 UV–vis spectrophotometer. PL spectra were measured with a Jasco FP-6300 spectrofluorometer. Single-crystal X-ray diffraction (XRD) data for dinitro compound **3** was collected on a Nonious CAD4 Kappa Axis XRD instrument and a Siemens Smart CCD XRD diffractometer, at room temperature (295 K), with graphite monochromated Mo K α radiation ($\lambda = 0.71073$ Å). Data were collected on the same instrument with ω scans with 2θ varied from 1.20 to 27.48°; 16,534 independent reflections measured; 6014 reflections were observed [$I > 2\sigma(I)$, where I = relative intensities and σ = the

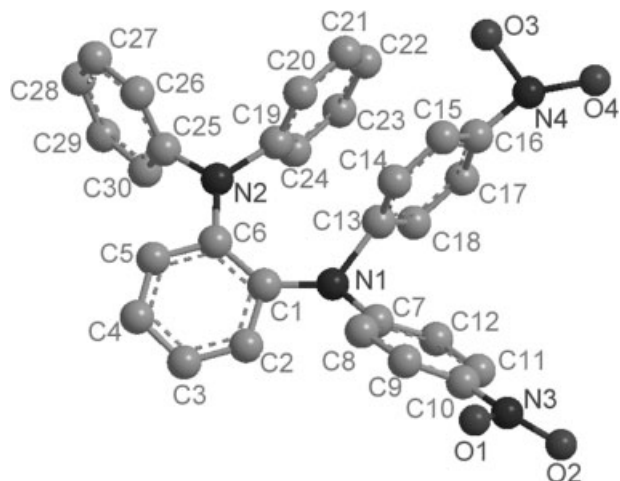


Figure 4. Molecular structure of dinitro compound **3** by single-crystal X-ray analysis.

net counting error]. The structure was solved with direct methods and was refined with standard techniques. A total of 344 parameters were varied in the final least squares.

RESULTS AND DISCUSSION

Monomer Synthesis

2 was prepared by the condensation of diphenylamine with 2-fluoronitrobenzene, followed by hydrazine Pd/C catalytic reduction according to the synthetic route outlined in Scheme 1.^{50–52} **4** was successfully synthesized by the amination reaction of **2** with 4-fluoronitrobenzene, followed by hydrazine Pd/C catalytic reduction. IR spectroscopy was used to identify the structures of the intermediate compounds **1**, **2**, and **3** and the diamine monomer **4**. The nitro groups of compounds **1** and **3** gave two characteristic bands around 1590 and 1356 cm^{-1} (NO_2 , asymmetric and symmetric stretching). After reduction, the characteristic absorptions of the nitro group disappeared, and the amino group showed the typical N–H stretching absorption pair in the region of 3300–3500 cm^{-1} . Figures 1–3 illustrate the ^1H and ^{13}C NMR spectra of the diamine compound **4**. The assignments of each carbon and proton are also given in these figures, and

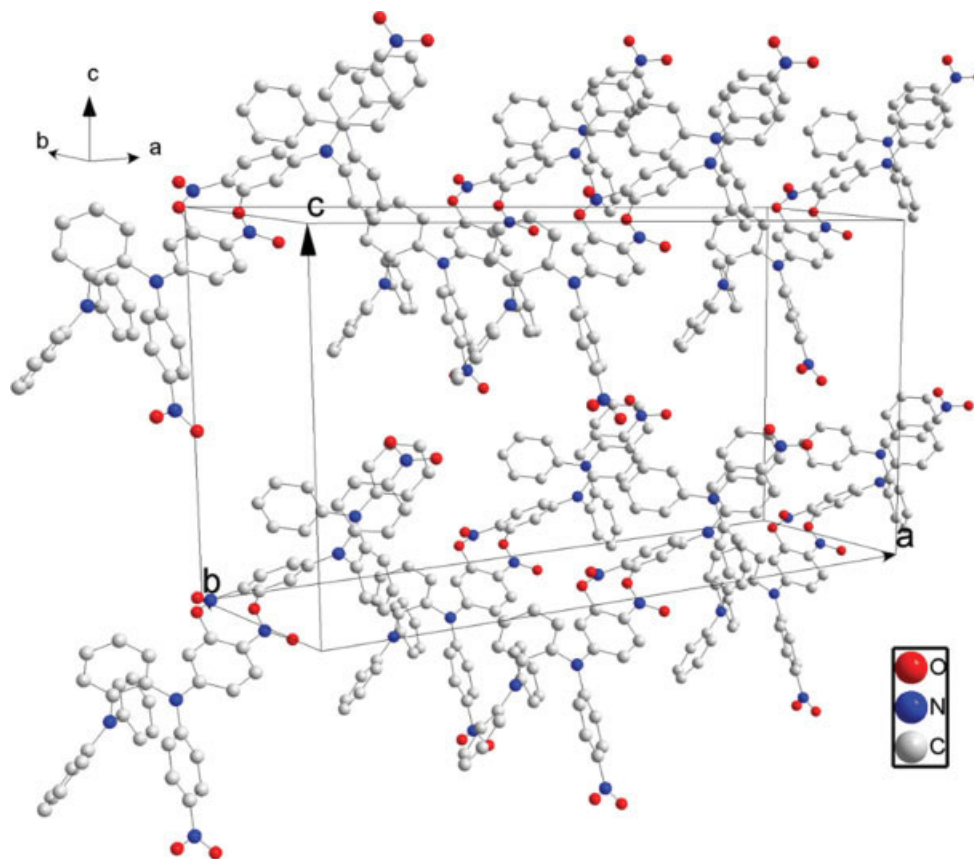


Figure 5. Unit cell for dinitro compound **3** by single-crystal X-ray analysis. [Color figure can be viewed in the online issue, which is available at www.interscience.wiley.com.]

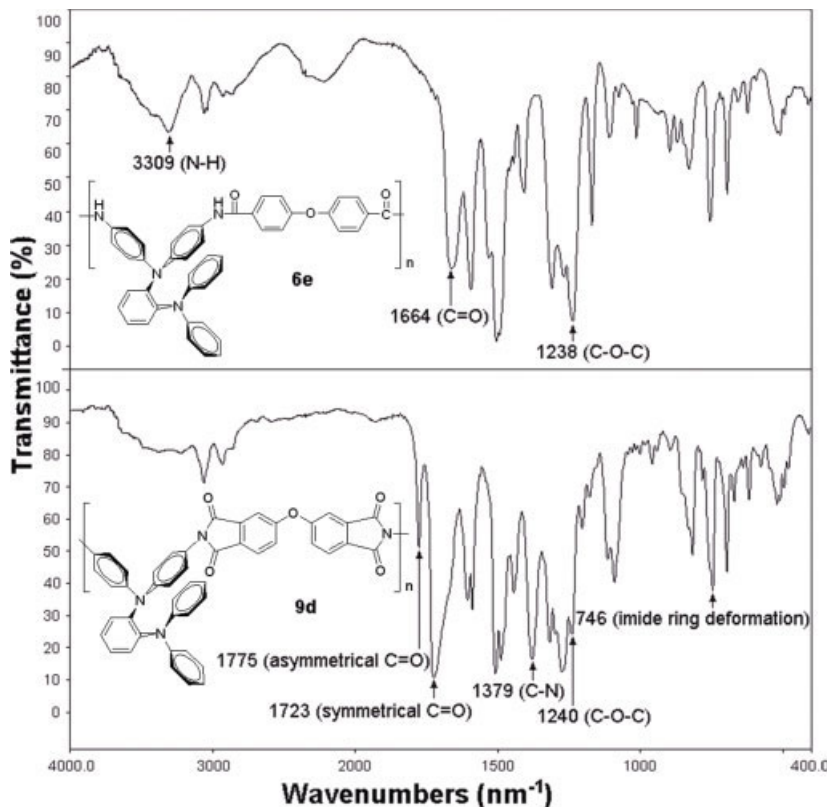


Figure 6. IR spectra (film) of poly(amine amide) **6e** and poly(amine imide) **9d**.

these spectra agree well with the proposed molecular structure. The ^1H NMR spectra confirm that the nitro groups have been completely transformed into amino groups by the high field shift of the aromatic protons and by the resonance signals around 4.65 ppm corresponding to the amino protons. The molecular structure of dinitro compound **3** was also confirmed by X-ray crystal analysis acquired from the single crystal obtained by slow crystallization of an acetonitrile solution of **3**. As shown in Figures 4 and 5, dinitro compound **3** displays a propeller-shaped configuration of the TPA cores, and the benzene rings are not in the same plane. This conformation will hinder the close packing of polymer chains and enhance the solubility of formed polymers.

Polymer Synthesis

The direct polycondensation technique was used for the synthesis of TPA-containing polyamides **6a–6h**, as shown in Scheme 1, from various combinations of monomers. First, the polyamides were prepared by the direct polycondensation of diamine **4** with various dicarboxylic acids (**5a–5h**) with TPP and Py as condensing agents. All the polymerizations pro-

ceeded homogeneously throughout the reaction and afforded viscous solutions, which precipitated in a tough, fiberlike form by the slow pouring of the resulting polymer solutions into methanol. Novel poly(amine imide)s **9a–9g** were synthesized by the conventional two-step method via a chemical imidization reaction, starting from diamine monomer **4** with tetracarboxylic dianhydrides **7a–7g** at room temperature (Scheme 1). Figure 6 shows typical IR spectra for poly(amine amide) **6e** and poly(amine imide) **9d**. These polymers exhibited characteristic amide absorption bands at 3309 (NH stretching) and 1664 cm^{-1} (C=O stretching) and imide absorption bands at 1775, 1723, and 742 cm^{-1} (imide ring deformation). Figure 7 shows a typical set of ^1H and ^{13}C NMR spectra of poly(amine amide) **6a** in $\text{DMSO-}d_6$, in which all the peaks have been readily assigned to the hydrogen and carbon atoms of the recurring unit.

Polymer Properties

Basic Characterization

The qualitative solubility properties of the polymers are presented in Table 1, and most of these

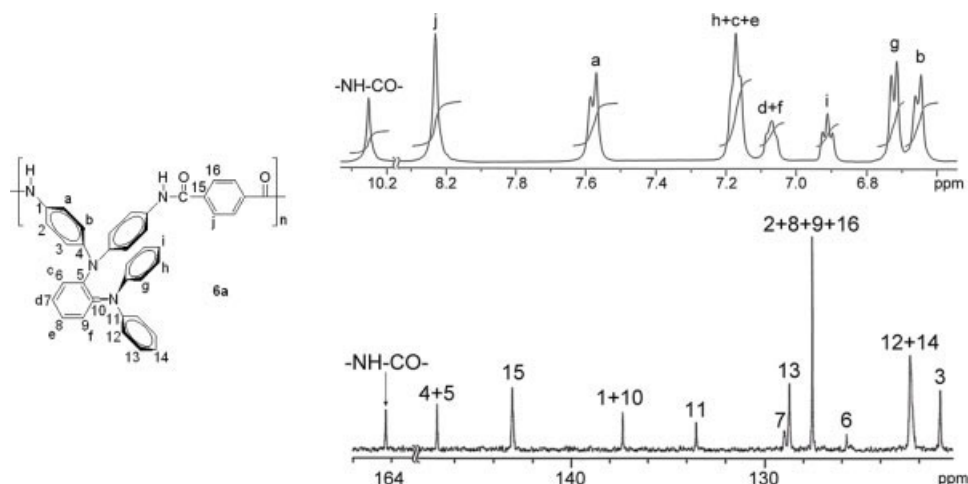


Figure 7. ^1H and ^{13}C NMR spectra of poly(amine amide) **6a** in $\text{DMSO-}d_6$.

polymers exhibited good solubility to highly polar organic solvents because of the introduction of the kink and bulky TPA core into the repeat unit.^{10,11} Thus, the excellent solubility makes these polymers potential candidates for practical applications by spin- or dip-coating processes to afford transparent and flexible films.

The thermal properties of all the obtained polymers were investigated by DSC. The results are summarized Table 2. All the polymers indicated no clear melting endotherms up to the decomposition
















temperatures on the DSC thermograms. This result supports the amorphous nature of the TPA-containing polymers.^{8–12} The T_g 's of these poly(amine amide)s and poly(amine imide)s were measured to be in the ranges of 174–292 and 271–311 °C, respectively, by DSC. The values are substantially higher than that of 4,4'-bis[*N,N*-(*m*-tolyl)phenylamino]biphenyl (63 °C), indicating that the use of these polymers may greatly improve the device durability, which is related to the T_g 's of the materials as reported by Tokito and coworkers.^{53,54}

Table 1. Solubility Behavior of the Aromatic Polymers^a

Polymer	Solubility						
	NMP	DMAc	DMF	DMSO	<i>m</i> -Cresol	THF	CHCl_3
6a	++	++	++	++	++	±	–
6b	++	++	++	++	++	±	–
6c	++	++	++	++	++	±	–
6d	++	++	++	++	++	±	–
6e	++	++	++	++	++	±	–
6f	++	++	++	++	++	±	–
6g	++	++	++	++	++	++	–
6h	++	++	++	++	++	–	–
9a	+	++	±	++	±	±	±
9b	++	±	±	+	+	+	++
9c	++	++	++	++	+	++	++
9d	++	+	++	++	+	++	++
9e	++	++	++	++	++	++	++
9f	++	++	++	+	+	++	++
9g	++	++	++	++	++	++	++

^a The solubility was determined with a 1-mg sample in 1 mL of a solvent. ++ = soluble at room temperature; + = soluble on heating; ± = partially soluble or swelling on heating; – = insoluble even on heating.

Table 2. Inherent Viscosity (η_{inh}) and Thermal Properties

Poly(amine amide)s 6a–6h				Poly(amine imide)s 9a–9g			
Code	Color of the Film	η_{inh} (dL/g) ^a	T_g (°C) ^b	Code	Color of the Film	η_{inh} (dL/g) ^a	T_g (°C) ^b
6a		0.38	292	9a		0.30	311
6b		0.28	274	9b		0.61	297
6c		0.36	277	9c		0.51	280
6d		0.64	261	9d		0.65	271
6e		0.58	281	9e		0.45	289
6f		0.23	286	9f		0.67	295
6g		0.14	174	9g		0.11	295
6h		0.31	211				

^a Measured at a polymer concentration of 0.5 g/dL in DMAc at 30 °C (**9a** was measured in concentrated sulfuric acid).

^b Midpoint temperature of the baseline shift on the second DSC heating trace (rate = 20 °C/min) of the sample after quenching from 400 °C.

[Color table can be viewed in the online issue, which is available at www.interscience.wiley.com.]

Optical and Electrochemical Properties

The optical and electrochemical properties of the poly(amine amide)s and poly(amine imide)s were investigated by CV, UV–vis, and PL spectroscopy. The results are summarized in Table 3. These polymers (**6a–6h** and **9a–9g**) exhibited strong UV–vis absorption bands at 270–315 and 301–318 nm in NMP solutions, which were assignable to the π – π^* transition resulting from the conjugation between the aromatic rings and nitrogen atoms. Their PL spectra in NMP solutions showed maximum bands around 406–465 and 396–451 nm in the violet-to-blue region. Figure 8 shows UV–vis absorption and PL spectra of polymers **6e**, **6g**, **6h**, and **9g** for comparison. The PL of the polymer solutions of **6a–6h** and **9a–9g**, and that of polymer thin films of **6g**, **6h**, and **9g** by UV irradiation (365 nm) are also shown in Figure 9. All the dilute polymer solutions and thin

films of **6g**, **6h**, and **9g** exhibited blue fluorescence. The polymer films were also measured for optical transparency with UV–vis spectroscopy. The UV–vis spectra of the polymer films and the cutoff wavelengths (absorption edge) from the UV–vis spectra are also indicated in Figure 10. It reveals that most of the visible light can be absorbed by poly(amine imide)s **9c** and **9e**, which show higher cutoff wavelengths. The selection of aliphatic or cycloaliphatic diacids and dianhydride monomers for this study was based on the anticipated structure–property relations for each type of nonaromatic group. Cycloaliphatic diacid or dianhydride imparts rigidity to the polymer backbone similar to that of aromatic monomers but offers improvements in polymer transparency and PL quantum yield because of the reduced formation of charge-transfer complexes and the extended conjugation structure,⁵⁵ both of which lead to the blueshift in the UV–vis cutoff-

Table 3. Optical and Electrochemical Properties of the Aromatic Polymers

Index	Solution λ (nm) ^a			Film λ (nm)			Oxidation (V; vs Ag/AgCl)		Band Gap (eV) ^g	HOMO (eV) ^f	LUMO (eV) ^g	
	Absorption Maximum	PL Maximum	Φ_{PL} (%) ^c	λ_0^d	Absorption Maximum ^b	Absorption Onset	PL Maximum	First				Second
								First				Second
6a	(295), 352 ^b	465	0.225	442	311	439	539	0.86	1.29	2.82	5.18	2.45
6b	(302), 342 ^b	465	0.309	415	317	408	506	0.87	1.27	3.04	5.19	2.15
6c	(300), 345 ^b	464	0.181	446	312	452	552	0.85	1.26	2.74	5.17	2.43
6d	(297), 352 ^b	451	0.282	446	314	430	533	0.84	1.17	2.88	5.16	2.28
6e	(270), 341 ^b	479	0.393	408	340	399	514	0.84	1.20	3.10	5.16	2.06
6f	(298) ^b	417	0.428	474	317	471	580	0.89	1.21	2.63	5.21	2.58
6g	(296) ^b	407	3.910	355	319	375	388	0.75	1.16	3.31	5.07	1.76
6h	(315) ^b	406	3.590	357	317	372	406	0.70	1.10	3.33	5.02	1.69
9a	(318) ^b	430	0.133	— ^h	322	381	— ⁱ	0.96	1.45	3.25	5.28	2.03
9b	(312) ^b	427	0.126	537	336	432	— ⁱ	1.00	1.46	2.87	5.32	2.45
9c	(309) ^b	428	0.402	568	311	379	— ⁱ	1.00	1.42	3.27	5.32	2.05
9d	(301) ^b	451	0.429	469	313	374	— ⁱ	0.98	1.40	3.31	5.30	1.99
9e	(305) ^b	436	0.470	552	307	383	— ⁱ	0.97	1.41	3.24	5.29	2.05
9f	(304) ^b	431	0.390	486	342	377	— ⁱ	1.01	1.42	3.29	5.33	2.04
9g	(301) ^b	396	1.780	376	314	370	382	0.99	1.38	3.35	5.31	1.96

^a UV-vis absorption measurements in NMP (1×10^{-5} M) at room temperature. The values in parentheses are the higher absorption values of the UV-vis λ_{max} solutions.

^b Excitation wavelength for PL and/or Φ_{PL} measurements.

^c PL quantum yield measured with quinine sulfate (dissolved in 1 N aqueous H₂SO₄ with a concentration of 10^{-5} M, assuming $\Phi_{\text{PL}} = 0.546$) as a standard at 24–25 °C].

^d Cutoff wavelength from the transmission UV-vis absorption spectra of the polymer films (polyimide thickness = 5–7 nm; polyimide thickness = 70–90 nm).

^e The data were calculated with the following equation: Gap = $1240/\lambda_{\text{abs,onset}}$.

^f The HOMO energy levels were calculated from CV and were referenced to ferrocene (4.8 eV).

^g LUMO = HOMO – Gap.

^h Polyimide **9a** formed an opaque film.

ⁱ No discernible λ_{PL} value was observed.

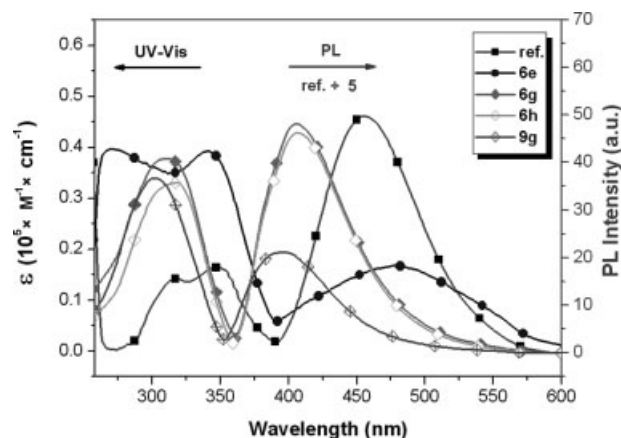


Figure 8. Molar absorptivity (ϵ) and PL of (■) quinine sulfate (ca. 1×10^{-5} M) in 1 N H_2SO_4 , (●) poly(amine amide) **6e**, (◆,◇) **6g** and **6h**, and (⊕) poly(amine imide) **9g** (ca. 1×10^{-5} M) in an NMP solution.

wavelength absorption (e.g., **6g**, **6h**, and **9g**). The wholly aromatic polymers therefore have strong absorptions in the visible region and in general are pale yellow or deep reddish-yellow because of their highly conjugated aromatic structures and/or the intermolecular charge-transfer complex formation.⁵⁶

The PL quantum yields of these polymers in NMP (ca. 1×10^{-5} M) were measured by comparison to quinine sulfate (ca. 1×10^{-5} M) in 1 N H_2SO_4 as a standard, and the results are summarized in Table 3. The quantum efficiencies of

these polymers after refractive index correction can be calculated according to eq 1:⁵⁷

$$\phi_{\text{unk}} = \phi_{\text{std}} \left(\frac{I_{\text{unk}}}{I_{\text{std}}} \right) \left(\frac{A_{\text{std}}}{A_{\text{unk}}} \right) \left(\frac{\eta_{\text{unk}}}{\eta_{\text{std}}} \right)^2 \quad (1)$$

where Φ_{unk} , Φ_{std} , I_{unk} , I_{std} , A_{unk} , A_{std} , η_{unk} , and η_{std} are the fluorescent quantum yields, the integrations of the emission intensities, the absorbances at the excitation wavelength, and the refractive indices of the corresponding solutions for the samples and the standard, respectively. Here we use the refractive indices of the pure solvents as those of the solutions. Assuming PL_{eff} of quinine sulfate in a 1 N H_2SO_4 solution to be 0.546 at 350 nm excitation,⁵⁸ the PL_{eff} values of these polyamides and polyimide dilute solutions in

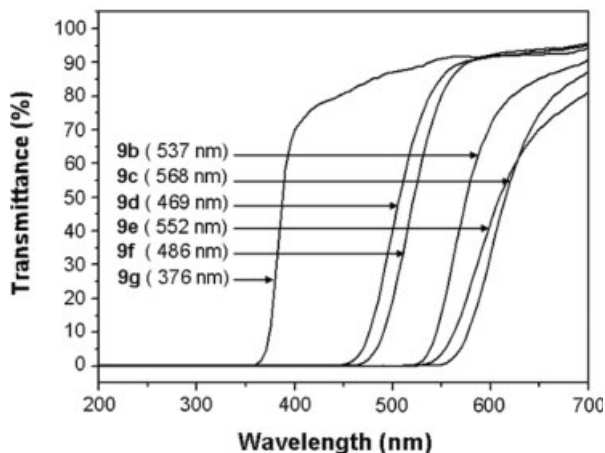
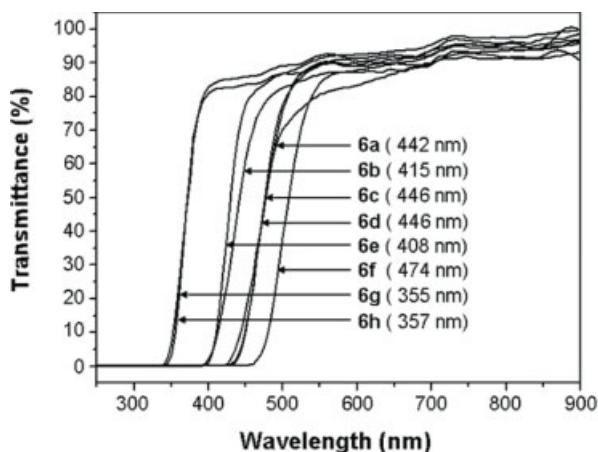


Figure 10. Transmission UV-vis absorption spectra of films (5–7 μm) of poly(amine amide)s **6a–6h** and of films (70–90 μm) of poly(amine imide)s **9b–9f**.

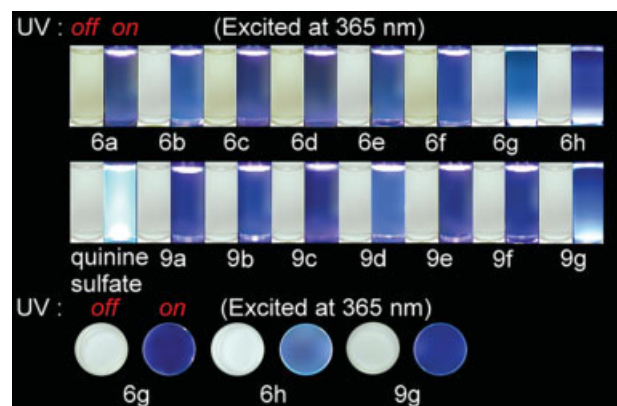


Figure 9. PL of polymer solutions **6a–6h** and **9a–9g** (10^{-5} M) in NMP and PL of polymer thin films **6g**, **6h**, and **9g** (thickness = 5–7 μm) by UV irradiation (excited at 365 nm). Quinine sulfate dissolved in 1 N aqueous H_2SO_4 (10^{-5} M) was used as the standard (PL quantum yield = 0.546).

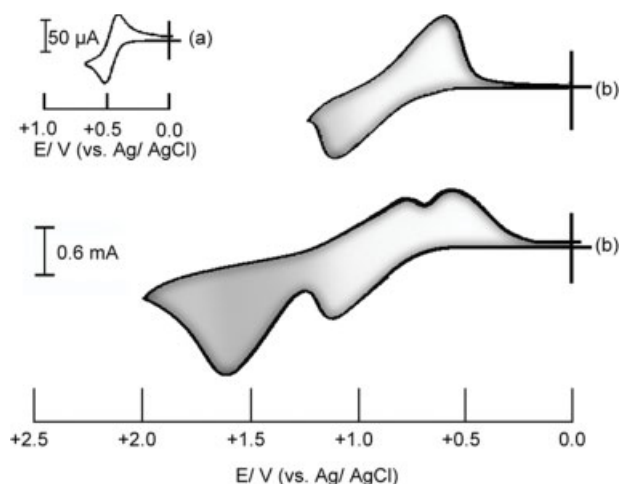
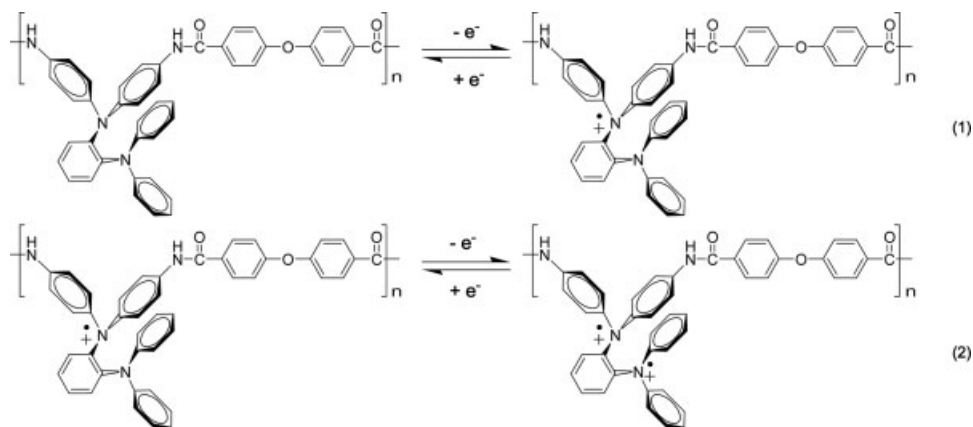


Figure 11. Cyclic voltammograms of (a) ferrocene and (b) a poly(amine amide) **6e** film on an ITO-coated glass substrate in CH_3CN containing 0.1 M TBAP. The scan rate was 0.1 V/s.

NMP were 3.910–0.181% and 1.780–0.126%, respectively. The quantum yields of polymers **6g**, **6h**, and **9g** were higher than those of the wholly aromatic polymers because of the reduced intermolecular charge-transfer effect.

The redox behavior was investigated with CV conducted for the cast film on an ITO-coated glass substrate as a working electrode in dry acetonitrile (CH_3CN) containing 0.1 M TBAP as an electrolyte under a nitrogen atmosphere. The typical cyclic voltammograms for poly(amine amide)s and poly(amine imide)s have two reversible oxidation redox couples at $E_{1/2}$, average potential of the redox couple peaks = 0.70–1.01 V and $E_{1/2} = 1.00$ –1.46 V. The typical cyclic voltammograms for polymer **6e** are shown in Figure 11. There are two reversible oxidation redox cou-

ples for poly(amine amide) **6e** at $E_{1/2} = 0.84$ V and $E_{1/2} = 1.20$ V corresponding to successive one-electron removal from the nitrogen atoms at the *N,N,N,N*-tetraphenyl-1,2-phenylenediamine structure in each repeating unit to yield one stable delocalized radical cation, poly(amine amide) $^{+\bullet}$ and one stable quinonoid-type dication, poly(amine amide) $^{2+}$, respectively.⁵⁹ The triarylamine centers at the *N,N,N,N*-tetraphenyl-1,2-phenylenediamine structures of the repeating unit are strongly coupled by the fact that the separation of the first and second oxidation redox couples is much larger than 35.6 mV.⁶⁰ Because of the good stability of the films and excellent adhesion between the polymer and ITO substrate, poly(amine amide) **6e** exhibited great reversibility of electrochromic characteristics by continuous five cyclic scans between 0.00 and 1.75 V, changing color from the original pale yellowish to green and then to blue. In addition, the first electron removal for poly(amine amide)s is assumed to occur at the nitrogen atom surrounded by amide groups, which is more electron-rich than the nitrogen atom surrounded by two phenyl groups without an electron-donating substituent. The energy of the highest occupied molecular orbital (HOMO) and lowest unoccupied molecular orbital (LUMO) levels of the investigated poly(amine amide)s and poly(amine imide)s can be determined from their oxidation half-wave potentials and the onset absorption wavelength, and the results are listed in Table 3. For example, the oxidation half-wave potential for poly(amine amide) **6e** has been determined to be 0.84 V versus Ag/AgCl. The external ferrocene/ferrocenium (Fc/Fc^+) redox standard $E_{1/2}$ value is 0.48 V versus Ag/AgCl in CH_3CN . Assuming that the HOMO energy for the Fc/Fc^+ standard is 4.80 eV with



Scheme 2

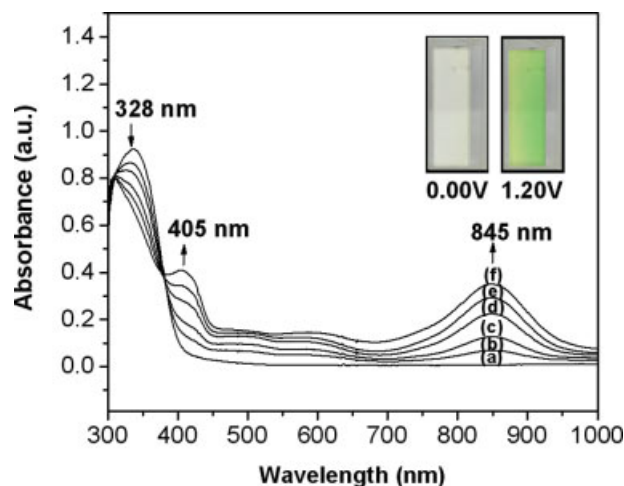


Figure 12. Electrochromic behavior of a poly(amine amide) **6e** thin film (in CH_3CN with 0.1 M TBAP as the supporting electrolyte) at (a) 0.00, (b) 0.84, (c) 0.96, (d) 1.05, (e) 1.11, and (f) 1.20 V. [Color figure can be viewed in the online issue, which is available at www.interscience.wiley.com.]

respect to the zero vacuum level, the HOMO energy for poly(amine amide) **6e** has been evaluated to be 5.16 eV.

Electrochromic Characteristics

Electrochromism of the thin films from poly(amine amide) **6e** was determined with an optically transparent thin-layer electrode coupled with UV-vis spectroscopy. The electrode preparations and solution conditions were identical to those used in CV. The typical electrochromic absorption spectra of poly(amine amide) **6e** are shown in Figures 12–14. When the applied potentials increased positively from 0 to 0.84 and then to 1.20 V, corresponding to the first and second electron oxidations, the peak of the characteristic absorbance at 328 nm for neutral-form poly(amine amide) **6e** decreased gradually, whereas two new bands grew up at 845 and 565 nm, respectively. The new spectral patterns were assigned as those of the cationic radical poly(amine amide)^{+•} and poly(amine amide)²⁺, respectively, by electron removal from the lone pair of electrons of the nitrogen atom on the *o*-phenylenediamine structures. According to the electron density between the two electroactive nitrogen atoms on the *o*-phenylenediamine structures in each repeating unit, the anodic oxidation pathway of poly(amine amide) **6e** was postulated as shown in Scheme 2. Meanwhile, the complemen-

tary color of the **6e** film changed from the original pale yellow to green (as shown in Fig. 12) and then to blue (as shown in Fig. 13) because of different oxidation states. Thus, this will be a good approach for facile color tuning of the electrochromic behaviors by the attachment of TPA units to the polymer main chain and/or as a pendant group.

The color switching times were estimated by the application of a potential step, and the absorbance profiles were followed. The switching time was defined as the time required to reach 90% of the full change in absorbance after switching the potential. Thin films from poly(amine amide) **6e** would require 7.5 s at 1.20 V for switching at 405 and 845 nm and 1.5 s for bleaching (Fig. 14). When the potential was set at 1.35 V, thin films from poly(amine amide) **6e** would require almost 9.5 s for coloration at 565 nm and 8 s for bleaching (Fig. 14). After five continuous cyclic scans between 0.0 and 1.75 V, the polymer films still exhibited excellent stability of the electrochromic characteristics.

CONCLUSIONS

A new TPA-containing aromatic diamine (**4**) was successfully synthesized in high purity and good yields. Novel aromatic poly(amine amide)s **6a–6h**

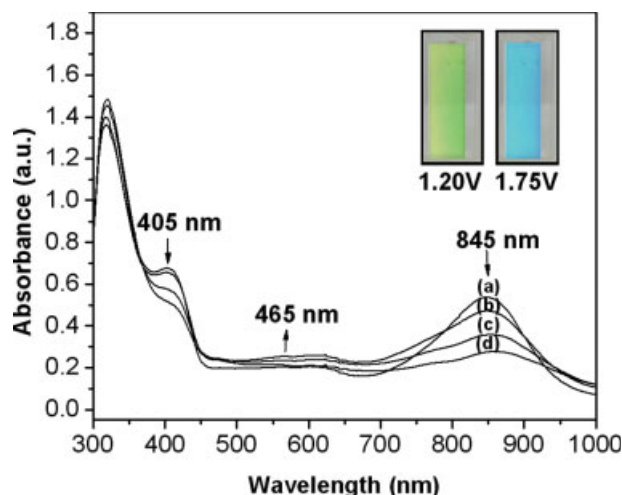


Figure 13. Electrochromic behavior of a poly(amine amide) **6e** thin film (in CH_3CN with 0.1 M TBAP as the supporting electrolyte) at (a) 1.20, (b) 1.41, (c) 1.62, and (d) 1.75 V. [Color figure can be viewed in the online issue, which is available at www.interscience.wiley.com.]

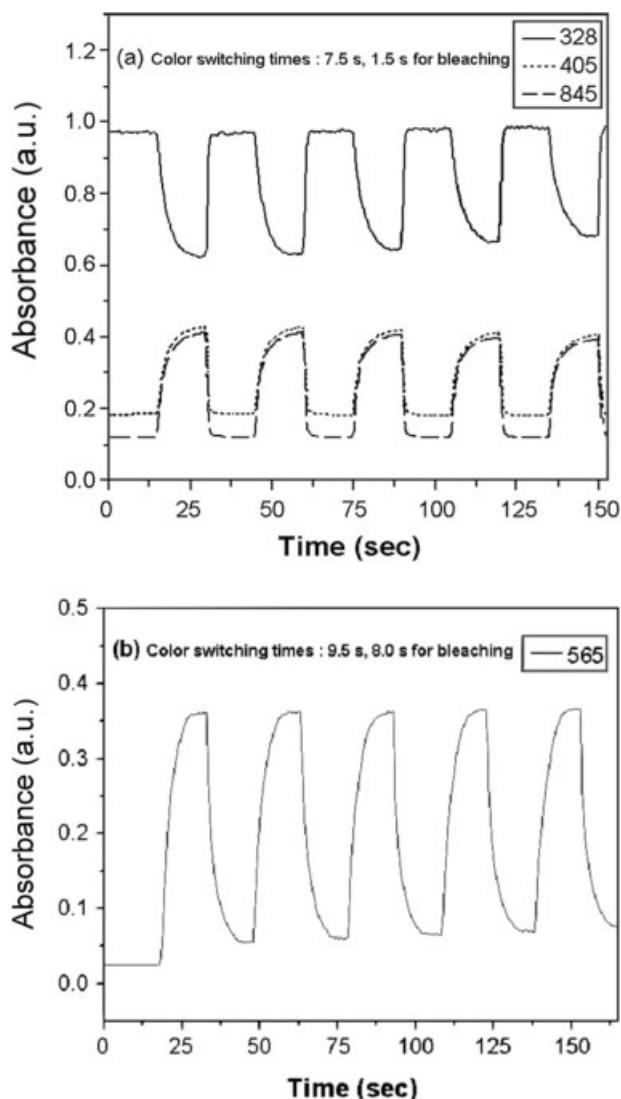


Figure 14. Potential step absorptometry of poly(amine amide) **6e** (in CH_3CN with 0.1 M TBAP as the supporting electrolyte) by the application of a potential step: (a) $0\text{ V} \leftrightarrow 1.20\text{ V}$ and (b) $0\text{ V} \leftrightarrow 1.75\text{ V}$.

and poly(amine imide)s **9a–9g** bearing pendent TPA groups were prepared from diamines with various aromatic diacids and aromatic tetracarboxylic dianhydride. The introduction of the bulky intrinsic electron-donating TPA group could increase the HOMO energy levels and disrupt the coplanarity of aromatic units in chain packing, and this increased the between-chain spaces or free volume and enhanced the solubility of the poly(amine amide)s and poly(amine imide)s. All the polymers were amorphous with good solubility in many polar aprotic solvents and exhibited excellent thin-film-forming ability.

In addition to high T_g values and good thermal stability, all the polymers also revealed excellent stability of the electrochromic characteristics by changing color from the original pale yellow to green and then to blue. Thus, these novel TPA-containing poly(amine amide)s and poly(amine imide)s may find applications in EL devices as HTL and electrochromic materials because of their proper HOMO values and excellent electrochemical and thermal stability.

The authors are grateful to the National Science Council of the Republic of China for its financial support of this work.

REFERENCES AND NOTES

1. Tang, C.-W.; VanSlyke, S.-A. *Appl Phys Lett* 1987, 51, 913.
2. Tang, C.-W.; VanSlyke, S.-A.; Chen, C.-H. *J Appl Phys* 1989, 65, 3610.
3. Adachi, C.; Nagai, K.; Tamoto, N. *Appl Phys Lett* 1995, 66, 2679.
4. Akcelrud, L. *Prog Polym Sci* 2003, 28, 875.
5. Shirota, Y. *J Mater Chem* 2000, 10, 1.
6. Shirota, Y. *J Mater Chem* 2005, 15, 75.
7. Bellmann, E.; Shaheen, S.-E.; Grubbs, R. H.; Marder, S.-R.; Kippelen, B.; Peyghambarian, N. *Chem Mater* 1999, 11, 399.
8. Lu, J.-P.; Hlil, A.-R.; Sun, Y.; Hay, A.-S.; Maindron, T.; Dodelet, J.-P.; D'Iorio, M. *Chem Mater* 1999, 11, 2501.
9. Wang, X.-Q.; Nakao, M.; Ogino, K.; Sato, H.; Tan, H. M. *Macromol Chem Phys* 2001, 202, 117.
10. Xiao, H.-B.; Leng, B.; Tian, H. *Polymer* 2005, 46, 5707.
11. Cho, J.-S.; Kimoto, A.; Higuchi, M.; Yamamoto, K. *Macromol Chem Phys* 2005, 206, 635.
12. Nomura, M.; Shibasaki, Y.; Ueda, M.; Tugita, K.; Ichikawa, M.; Taniguchi, Y. *Macromolecules* 2004, 37, 1204.
13. Sun, M.-H.; Li, J.; Li, B.-S.; Fu, Y.-Q.; Bo, Z.-S. *Macromolecules* 2005, 38, 2651.
14. Liu, Y.-Q.; Liu, M.-S.; Li, X.-C.; Jen, A. K.-Y. *Chem Mater* 1998, 10, 3301.
15. Li, X.-C.; Liu, Y.-Q.; Liu, M.-S.; Jen, A. K.-Y. *Chem Mater* 1999, 11, 1568.
16. Redecker, M.; Bradley, D.-D.-C.; Inbasekaran, M.; Wu, W.-W.; Woo, E.-P. *Adv Mater* 1999, 11, 241.
17. Ego, C.; Grimsdale, A.-C.; Uckert, F.; Yu, G.; Srdanov, G.; Mullen, K. *Adv Mater* 2002, 14, 809.
18. Kim, Y.-H.; Zhao, Q.; Kwon, S.-K. *J Polym Sci Part A: Polym Chem* 2006, 44, 172.
19. Wang, H.; Li, Z.; Jiang, Z.; Ligang, Y.; Wang, H.; Qin, J.; Yu, G.; Liu, Y. *J Polym Sci Part A: Polym Chem* 2005, 43, 493.

20. Li, H.; Hu, Y.; Zhang, Y.; Ma, D.; Wang, L.; Jing, X.; Wang, F. *J Polym Sci Part A: Polym Chem* 2004, 42, 3947.
21. Sung, H.-H.; Lin, H.-C. *J Polym Sci Part A: Polym Chem* 2005, 43, 2700.
22. Pu, Y.-J.; Soma, M.; Kido, J.; Nishide, H. *Chem Mater* 2001, 13, 3817.
23. Liang, F.-S.; Pu, Y.-J.; Kurata, T.; Kido, J.; Nishide, H. *Polymer* 2005, 46, 3767.
24. Liang, F.-S.; Kurata, T.; Nishide, H.; Kido, J. *J Polym Sci Part A: Polym Chem* 2005, 43, 5765.
25. Hsiao, S.-H.; Chen, C.-W.; Liou, G.-S. *J Polym Sci Part A: Polym Chem* 2004, 42, 3302.
26. Miteva, T.; Meisel, A.; Knoll, W.; Nothofer, H.-G.; Scherf, U.; Muller, D.-C.; Meerholz, K.; Yasuda, A.; Neher, D. *Adv Mater* 2001, 13, 565.
27. Fu, Y.-Q.; Li, Y.; Li, J.; Yan, S.-K.; Bo, Z.-S. *Macromolecules* 2004, 37, 6395.
28. Polyimides; Wilson, D.; Stenzenberger, H.-D.; Hergenrother, P.-M., Eds.; Blackie: Glasgow, 1990.
29. Polyimides: Fundamentals and Applications; Ghosh, M.-K.; Mittal, K.-L., Eds.; Marcel Dekker: New York, 1996.
30. Liaw, D. *J Polym Sci Part A: Polym Chem* 2005, 43, 4559.
31. Harris, F.-W.; Hsu, S. L.-C. *High Perform Polym* 1989, 1, 1.
32. Imai, Y. *React Funct Polym* 1996, 30, 3.
33. Hsiao, S.-H.; Li, C.-T. *Macromolecules* 1998, 31, 7213.
34. Liou, G.-S. *J Polym Sci Part A: Polym Chem* 1998, 36, 1937.
35. Eastmond, G.-C.; Paprotny, J.; Irwin, R.-S. *Polymer* 1999, 40, 469.
36. Eastmond, G.-C.; Gibas, M.; Paprotny, J. *Eur Polym J* 1999, 35, 2097.
37. Reddy, D.-S.; Chou, C.-H.; Shu, C.-F.; Lee, G.-H. *Polymer* 2003, 44, 557.
38. Myung, B.-Y.; Ahn, C.-J.; Yoon, T.-H. *Polymer* 2004, 45, 3185.
39. Zhang, F.; Jia, Z.; Srinivasan, M.-P. *Langmuir* 2005, 21, 3389.
40. Liaw, D.-J.; Chang, F.-C.; Leung, M.-K.; Chou, M.-Y.; Muellen, K. *Macromolecules* 2005, 38, 4024.
41. Liou, G.-S.; Hsiao, S.-H.; Ishida, M.; Kakimoto, M.; Imai, Y. *J Polym Sci Part A: Polym Chem* 2002, 40, 2810.
42. Liou, G.-S.; Hsiao, S.-H.; Ishida, M.; Kakimoto, M.; Imai, Y. *J Polym Sci Part A: Polym Chem* 2002, 40, 3815.
43. Su, T.-H.; Hsiao, S.-H.; Liou, G.-S. *J Polym Sci Part A: Polym Chem* 2005, 43, 2085.
44. Cheng, S.-H.; Hsiao, S.-H.; Su, T.-H.; Liou, G.-S. *Macromolecules* 2005, 38, 307.
45. Liou, G.-S.; Hsiao, S.-H.; Su, T.-X. *J Mater Chem* 2005, 15, 1812.
46. Liou, G.-S.; Hsiao, S.-H.; Su, T.-X. *J Polym Sci Part A: Polym Chem* 2005, 43, 3245.
47. Seo, E.-T.; Nelson, R.-F.; Fritsch, J.-M.; Marcoux, L.-S.; Leedy, D.-W.; Adams, R. N. *J Am Chem Soc* 1966, 88, 3498.
48. Chiu, K.-Y.; Su, T.-X.; Li, J. H.; Lin, T.-H.; Liou, G.-S.; Cheng, S.-H. *J Electroanal Chem* 2005, 575, 95.
49. Chiu, K.-Y.; Su, T.-H.; Huang, C.-W.; Liou, G.-S.; Cheng, S.-H. *J Electroanal Chem* 2005, 578, 283.
50. Gujadhur, R.; Venkataraman, D.; Kintigh, J.-T. *Tetrahedron Lett* 2001, 42, 4791.
51. Uргаonkar, S.; Xu, J.-H.; Verkade, J.-G. *J Org Chem* 2003, 68, 8416.
52. Bergstrom, F.-W.; Granara, I.-M.; Erickson, V. *J Org Chem* 1942, 7, 98.
53. Tokito, S.; Tanaka, H.; Okada, A.; Taga, Y. *Appl Phys Lett* 1996, 69, 878.
54. Tokito, S.; Tanaka, H.; Noda, K.; Okada, A.; Taga, Y. *Appl Phys Lett* 1997, 70, 1929.
55. Hasegawa, M.; Horie, K. *Prog Polym Sci* 2001, 26, 259.
56. Matsumoto, T.; Kurosaki, T. *Macromolecules* 1997, 30, 993.
57. Xue, C.; Chen, Z.; Wen, Y.; Luo, F.-T.; Chen, J.; Liu, H. *Langmuir* 2005, 21, 7860.
58. Demas, J.-N.; Crosby, G.-A. *J Phys Chem* 1971, 75, 991.
59. Selby, T.-D.; Kim, K.-Y.; Blackstock, S.-C. *Chem Mater* 2002, 14, 1685.
60. Lambert, C.; Noll, G. *J Am Chem Soc* 1999, 121, 8434.